

Supplemental Material for: ‘Thermodynamically limited Cu-Zn order $\text{Cu}_2\text{ZnSnS}_4$ (CZTS) from Monte Carlo simulations’

Suzanne K. Wallace^{a,b}, Jarvist Moore Frost^{a,b}, and Aron Walsh^{*b,c}

^a *Department of Chemistry, Centre for Sustainable Chemical Technologies, University of Bath, Claverton Down, Bath, BA2 7AY, UK*

^b *Department of Materials, Imperial College London, Exhibition Road, London SW7 2AZ, UK. Email: a.walsh@imperial.ac.uk*

^c *Global E³ Institute and Department of Materials Science and Engineering, Yonsei University, Seoul 03722, Korea*

1 Convergence of change in lattice energy with cut off radius for Monte Carlo moves *check with Jarv*

In our Monte Carlo (MC) simulations, we use the change in lattice energy, ΔE , of the system before and after performing a MC move (nearest-neighbour Cu-Zn substitution) to determine if the move should be accepted or rejected. In a simple model of ionic crystals, it is assumed that U is given entirely by the potential energy of classical ions localised at the equilibrium positions [2]. The ions are regarded as point charges within a regular 3D array. The forces holding the ions together are assumed to be electrostatic and so can be calculated by the summation of all of the electrostatic attractions and repulsions in the crystal. Two oppositely charged ions separated by a distance r experience an attractive Coulomb force, F , shown in equation 1. Their Coulombic potential energy, V , is then given by equation 2 [10].

$$F = \frac{e^2 Z_+ Z_-}{4\pi\epsilon_0 r^2} \quad (1)$$

$$V = \int_{\infty}^r F dr = -\frac{e^2 Z_+ Z_-}{4\pi\epsilon_0 r} \quad (2)$$

Considering nearest neighbouring ions, next-nearest neighbours, etc. out to a particular cut off and summing over all of the contributions to the electrostatic potential gives the first term in the expression for the total lattice energy, U , in equation 3, where A is the Madelung constant and N is the number of ions per mole. The Madelung constant depends only on the geometrical arrangement of point charges and so has the same value for all compounds with the same structure type [10]. To

obtain the total energy of the crystal, U , short-range repulsive forces usually must also be accounted for. These forces become important when ions are close enough that their electron clouds begin to overlap. Repulsive forces are given by the second term in equation 3, where B is a constant and n is in the range 5 to 12 [10]. However, in our on-lattice calculations of disorder we omit the term for short-range repulsive forces in the lattice energy because the ions are fixed on lattice points and so their electron clouds will never be allowed to overlap. We also only consider nearest neighbours when we compute the first term in equation 3.

$$U = -\frac{e^2 Z_+ Z_-}{4\pi\epsilon_0 r} N A + \frac{BN}{r^n} \quad (3)$$

As we are interested in obtaining the change in lattice energy, ΔE , we also do not compute all contributions to the lattice energy in the system. Instead, we consider contributions out to a finite radius about the particular site our trial move proposes swapping. This is illustrated by the schematic in Fig. 1. To ensure that we have use a suitable r_{cutoff} for our lattice summations when calculating ΔE for each MC move, we calculate ΔE for the same move with increasing r_{cutoff} , as shown in Fig. 1. From this, we have taken 5 lattice units as a suitable value for r_{cutoff} .

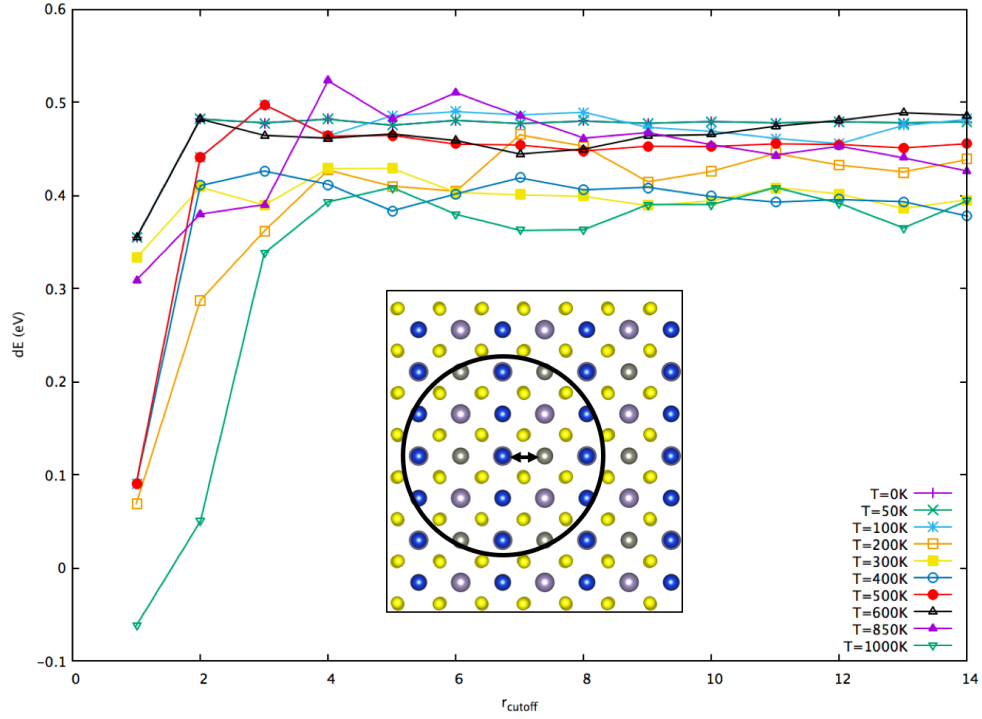


Figure 1: Convergence in the change in lattice energy (ΔE) with respect to the cut-off radius (r_{cutoff}) for the lattice summations. Schematic shows a proposed swap between a Cu (blue) and Zn (steel grey) ion, and the circle is used to demonstrate a cut off radius used for the lattice energy summation for the ΔE .

2 Convergence in lattice potential with cut off radius for equilibration test

We take a value of 10 lattice units as suitable r_{cutoff} for lattice potential calculation in equilibration test using variance in distribution of Sn potentials calculated with our custom code based on Fig. 2.

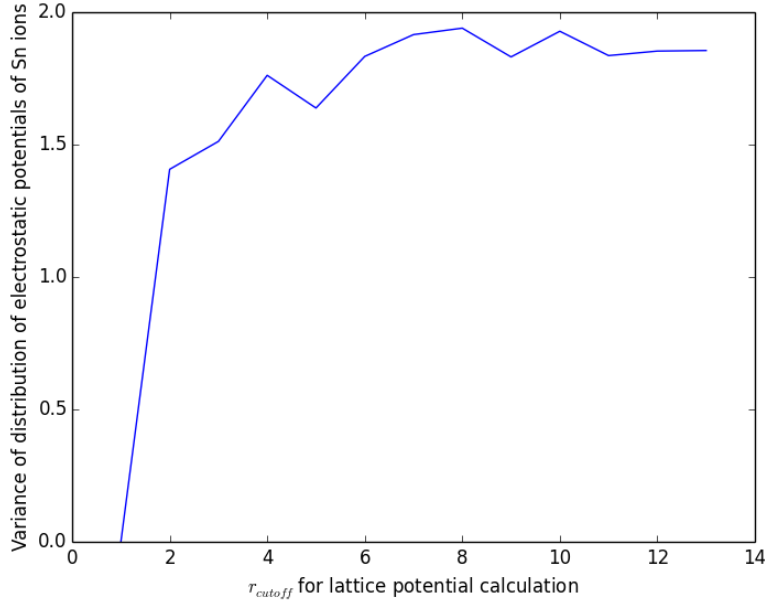


Figure 2: Convergence in the variance of the distribution of on-site electrostatic potentials of Sn ions calculated by our custom code with increasing cut-off radius for each calculation of lattice potential. Simulation run at $T=1050K$ and allowed to evolve from an ordered initial lattice.

3 First principles calculation of the formation energy of the $[Cu_{Zn}^- + Zn_{Cu}^+]$ defect pair in Cu_2ZnSnS_4

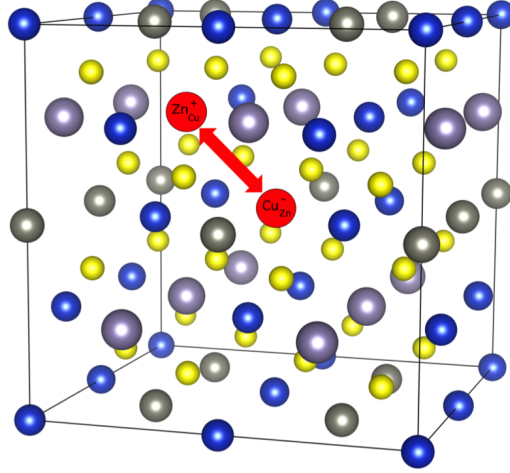


Figure 3: 64 atom supercell of Cu_2ZnSnS_4 showing a substitution of Cu and Zn ions that results in the formation of the nearest neighbour antisite defect pair.

In our calculation of Cu_{Zn}^- and Zn_{Cu}^+ antisite defects in Cu_2ZnSnS_4 (CZTS) we use a 64 atom supercell, which is the most isotropic and largest supercell that could feasibly be used for our calculations at the level of accuracy we required. This corresponds to a cell size of approximately $11 \times 11 \times 11 \text{ \AA}^3$. This supercell is constructed by creating a $2 \times 2 \times 1$ supercell of the conventional unit cell of CZTS. For our calculation of the formation energy of the nearest-neighbour $[Cu_{Zn}^- + Zn_{Cu}^+]$ defect pair (shown in figure 3), we make use of the Heyd-Scuseria-Ernzerhof (HSE06) hybrid-functional [3] for the exchange-correlation functional as implemented in the Vienna Ab-initio Simulation Package (VASP) [4, 5]. This functional mixes 25% of screened Hartree-Fock ex-

change to the Perdew-Burke-Ernzerhof (PBE) exchange functional [8]. Projector augmented-wave potentials [6] were used to describe the core electrons with an energy cut-off of 500 eV for the plane-wave basis set. Calculations were initially performed at the gamma point (a $1 \times 1 \times 1$ k -point mesh) until forces on the ions converged to within 0.01 eV/Å. A single geometry step was then performed with a $2 \times 2 \times 2$ k -point mesh centred on the gamma point as these parameters were found to be sufficient for the total energy to converge to within <2 meV per atom with respect to increased plane-wave cut-off energy and for the external pressure to be <1 kbar. However, performing the full calculation with a $2 \times 2 \times 2$ k -point mesh was found to be too computationally expensive. Data for the convergence test is given in table 1.

Cut-off energy (eV)	k -points	Total energy, E (eV)	External pressure (kbar)	dE per atom (meV)
300	$1 \times 1 \times 1$	-305.53	-174.59	
350	$1 \times 1 \times 1$	-306.95	-23.86	- 22.12
400	$1 \times 1 \times 1$	-307.49	8.21	- 8.47
450	$1 \times 1 \times 1$	-307.08	5.71	6.33
500	$1 \times 1 \times 1$	-307.20	4.02	- 1.87
300	$2 \times 2 \times 2$	-306.76	-180.97	
500	$2 \times 2 \times 2$	-308.72	-0.08	

Table 1: Convergence tests performed on the perfect CZTS supercell with various plane wave cut-off energies for the basis set and number of k -points in the sampling where dE is the difference in the total energy obtained as the cut-off energy for the plane-wave basis set is increased in increments of 50 eV.

The full expression for the formation energy of a defect is given in equation 4, where $\Delta H_{D,q}$ is the total energy of the su-

percell containing the defect in charge state q , E_H is the total energy of an equivalent supercell of the perfect host crystal without the defect. The chemical potential μ_α describes the energy of the atomic reservoir of the atoms α removed from or added to the host crystal when the defect forms. For charged defects, where $q \neq 0$, E_F describes the energy of the reservoir of electrons, which is usually considered to be somewhere between the valence band maximum and conduction band minimum, but can be tuned by an applied bias. However, in the case of the anti-site pair $[Cu_{Zn}^- + Zn_{Cu}^+]$, we do not add or remove any atoms, we only substitute their positions. Also the defect complex is overall charge neutral and so the full expression simplifies to that shown in equation 5. From our calculation, we predict a defect formation energy of 0.30 eV.

$$\Delta H_{D,q}(E_F, \mu) = [E_{D,q} - E_H] + \sum_{\alpha} n_{\alpha} \mu_{\alpha} + q \cdot E_F \quad (4)$$

$$\Delta H_D = E_{D,q} - E_H \quad (5)$$

First principles calculations using the density function theory (DFT) formalism have been found to yield reliable information about atomic structure, including the relaxation of the host atoms, during the formation of a defect in a crystal. However, in many cases traditional DFT functionals used in standard DFT methods often fail at the description of the electronic structure of a defective crystal. For instance, the local density approximation (LDA) and generalized gradient approximation (GGA), severely underestimate the band gaps of semiconductors and insulators [1]. Defect formation energies are in general affected by this band-gap problem in two ways. Firstly, defect states may be predicted to be within the continuum of host states when the band gap is underestimated but actually be within the band

gap if the band-gap problem is corrected. The result of this incorrect placement of the defect level is that electron-occupied defect states can erroneously spill into the conduction band or similarly hole defects could spill into the valence band. The calculated charge density associated with these defects would then be incorrect, resulting in an uncontrolled error in the value obtained for $\Delta H_{D,q}$. For charged defects, there is an additional source of error due to $\Delta H_{D,q}$ being dependent upon the Fermi level. E_F is bounded by the band-edge energies and so when the band gap is changed the range of formation energies between the valence band maximum and conduction band minimum is altered [7]. The band gap problem can be addressed by going beyond DFT. One such method is hybrid-DFT. Hybrid approaches incorporate a certain amount of screened exact exchange from the Hartree-Fock approximation with DFT exchange-correlation functionals. Hybrid functionals, such as the HSE06 functional [3] used in this study have been shown to produce band structures in much better agreement with experiment and provide a much more reliable description of charge localization, which is essential for accurate modeling of low-symmetry defects or structures that give rise to polaron formation [1].

When defect concentrations are less than 1%, it is usually assumed that the system is in the dilute defect limit where defects can be considered to be non-interacting. Using statistical thermodynamics for point defects, an expression for the equilibrium concentration of point defects as a function of temperature can be obtained [9]. This is shown in equation 6, where N is the number of sites, ΔH is the defect formation energy, k_B is the

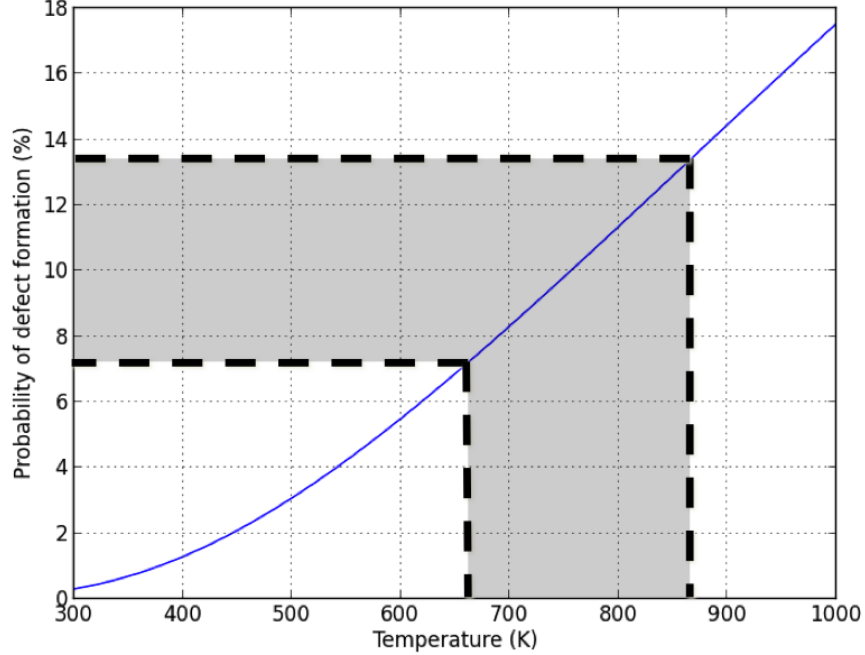


Figure 4: Probability of nearest neighbour $[Cu_{Zn}^- + Zn_{Cu}^+]$ defect formation as a function of temperature based on the equilibrium defect concentration from classical thermodynamics. The shaded region indicates typical annealing temperatures used in the synthesis of Cu_2ZnSnS_4 .

Boltzmann constant and T is the temperature of the system.

$$n = Ne^{\frac{-\Delta H}{k_B T}} \quad (6)$$

The probability of defect formation as a function of temperature is given by the exponential expression in equation 6. The defect formation energy from the DFT calculations were halved to take an average of the formation energy per defect during the formation of an antisite pair before being inserted into this expression. This is plotted against temperature in figure 4.

It can be seen from figure 4 that the probability of defect formation at a typical annealing temperatures is approximately 7-13%. It was also found that, compared to the undefective system, there was a decrease in the separation of the antisite defects of 3.84\AA to 3.82\AA after the geometry optimization. This effect could be due to a Coulombic attraction between the two antisite defects. The point defects (the Cu_{Zn}^- and Zn_{Cu}^+ antisites) form the defect complex $[Cu_{Zn}^- + Zn_{Cu}^+]$. The point defects become associated with one another due to a Coulomb interaction between the effective +1 and -1 charge that results from substituting species with a +1 charge with a species with a +2 charge and vice versa. This, in addition to the high equilibrium concentrations of antisite defects predicted, suggests that it is not sufficient to consider the Cu_{Zn}^- and Zn_{Cu}^+ antisites as non-interacting point defects and that we must instead consider a system of interacting defects. We aim to do this through our Monte Carlo simulations of thermodynamic disorder.

References

- [1] A. Alkauskas, M. D. McCluskey, and C. G. Van de Walle. Tutorial: Defects in semiconductors - Combining experiment and theory. *Journal of Applied Physics*, 119(18):181101, 2016.
- [2] N. Ashcroft and N. Mermin. *Cohesive Energy*. Saunders College Publishing, 1976.
- [3] J. Heyd, G. E. Scuseria, and M. Ernzerhof. Hybrid functionals based on a screened Coulomb potential. *Journal of Chemical Physics*, 118(18):8207–8215, 2003.
- [4] G. Kresse and J. Furthmüller. Efficiency of ab-initio total energy calculations for metals and semiconductors using a plane-wave basis set. *Computational Materials Science*, 6(1):15–50, 1996.
- [5] G. Kresse and J. Furthmüller. Efficient iterative schemes for ab initio total-energy calculations using a plane-wave basis set. *Physical Review B*, 54(16):11169–11186, 1996.
- [6] G. Kresse and D. Joubert. From ultrasoft pseudopotentials to the projector augmented-wave method. *Physical Review B*, 59:1758–1775, 1999.
- [7] S. Lany and A. Zunger. Accurate prediction of defect properties in density functional supercell calculations. *Model. Simul. Mater. Sci. Eng.*, 17(8):084002, 2009.
- [8] J. P. Perdew, K. Burke, and M. Ernzerhof. Generalized gradient approximation made simple. *Physical Review Letters*, 77:3865–3868, 1996.

- [9] P. Varotsos and K. Alexopoulos. *Thermodynamics of Point Defects and Their Relation with Bulk Properties*. North-Holland Physics Publishing, 1986.
- [10] A. West. *Bonding in Solids*. John Wiley & Sons, Ltd., 1999.